Supplemental data for "TELP, a sensitive and versatile library construction method for next-generation sequencing" by Peng, X., et.al., NAR, 2014.

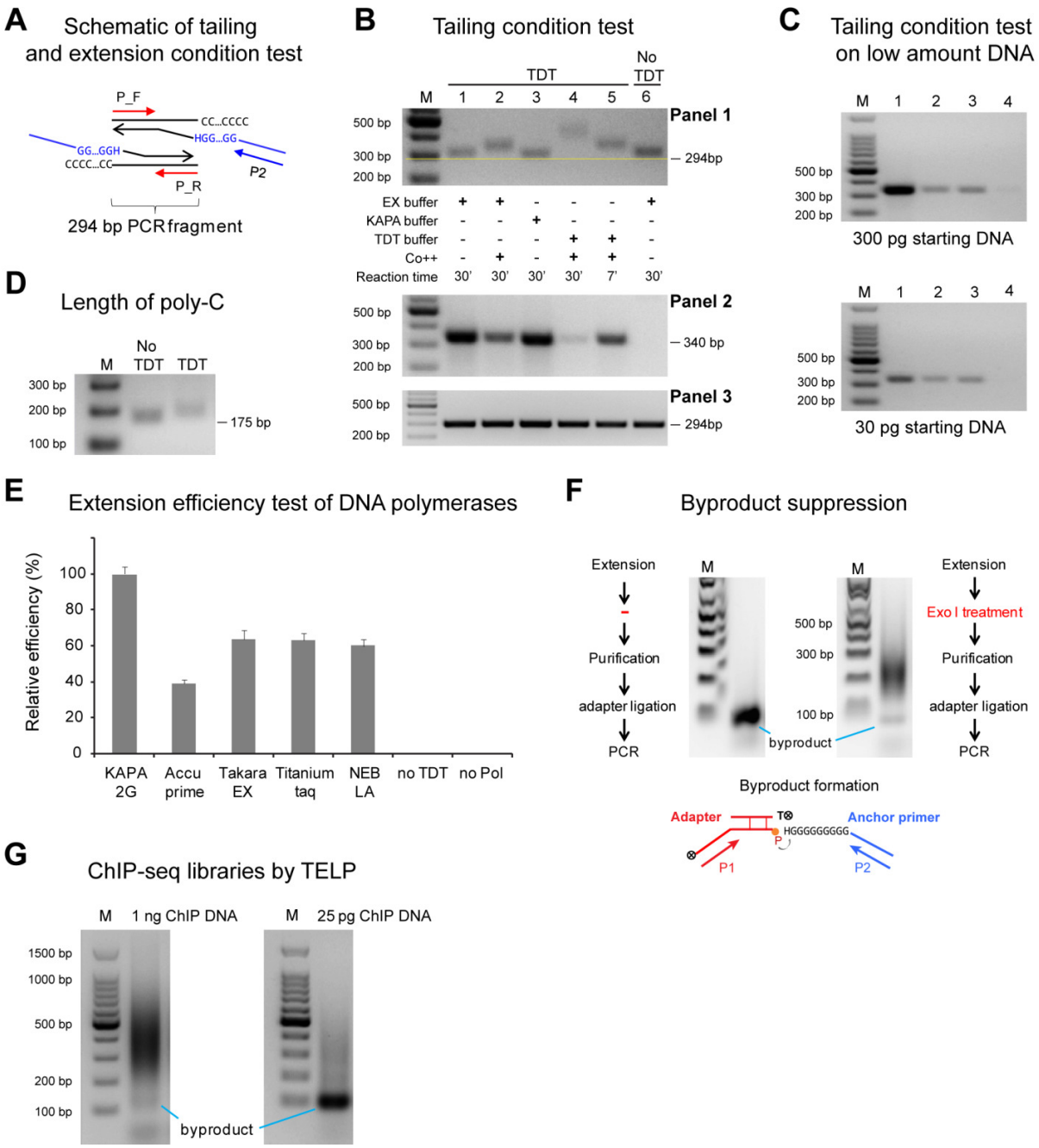

Figure S1. Development of the TELP sequencing library construction method.

(A) A schematic of the tests for the tailing and extension conditions. A 294-bp PCR fragment was used to optimize the tailing and extension conditions. First, a poly-C tail was added to this PCR fragment using TDT under various conditions. Then, an extension reaction was performed using five different DNA polymerases. The efficiencies of tailing and extension were evaluated by examining the amount of final extension product through PCR using primers P_F and P2. The amount of original DNA was evaluated through PCR using primers P_F and P_R and was used as an internal control. **(B)** In this test, the extension conditions were fixed to evaluate the influence of the length of the poly-C tail on the final yield of the extension product. We aimed to identify the tailing conditions that provide the highest yield of the final extension product. Panel 1 shows the tailing efficiency of TDT under various conditions as indicated under the gel image. The amount of the final extension product was examined through PCR using primers P_F and P2 (amplicon size, 340 bp), as shown in Panel 2. Panel 3 shows the amount of the original DNA as evaluated by PCR using primers P_F and P_R. **(C)** Test of tailing conditions on 300 pg and 30 pg starting DNA. Conditions 1 through 4 were the same as in (B). **(D)** Tailing was performed on a 175-bp PCR fragment under condition 1 in (B) to estimate the length of poly-C. **(E)** In this test, the tailing condition was fixed [condition 1 in (B)] to evaluate the extension efficiency of various DNA polymerases. The final extension product was quantified through real-time PCR using primers P_F and P2 and then normalized to the internal control amplified with primers P_F and P_R. These results are the averages of three independent experiments, and the error bars indicate standard deviations. **(F)** A comparison of byproduct formation with or without exonuclease I digestion after the extension step. The byproduct structure is illustrated below the gel image. **(G)** TELP sequencing libraries constructed from 1 ng and 25 pg ChIP DNA. Byproduct formation was compared between the two libraries generated from normal (1 ng) and low (25 pg) amounts of ChIP DNA.

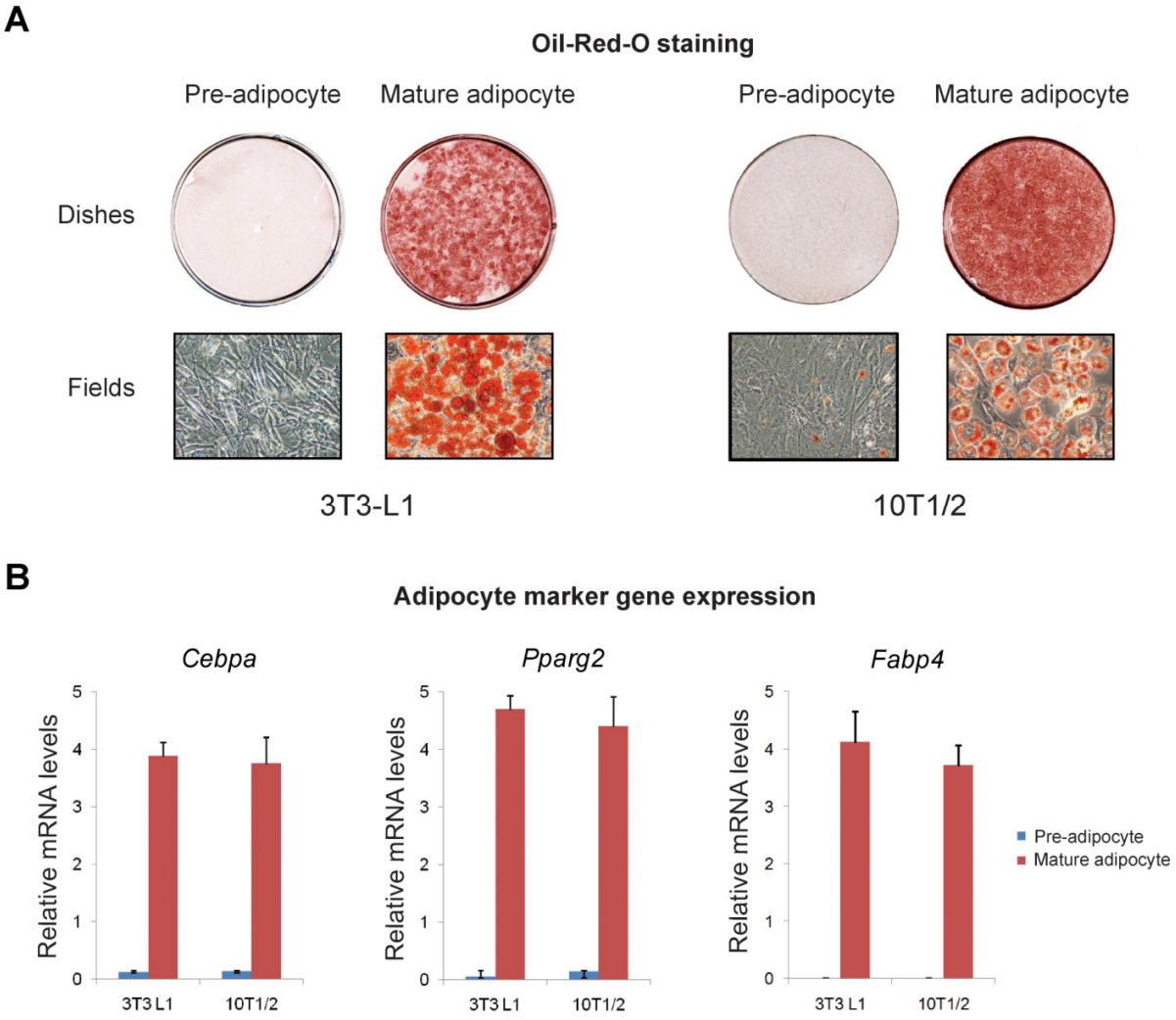

Figure S2. *In vitro* differentiation of the murine adipocyte precursor cells.
(A) Oil-Red-O staining of preadipocytes and mature adipocytes derived from the mouse adipocyte precursor cell 3T3-L1 and the multi-potent mesenchymal stem cell C3H 10T1/2. Top panels, stained dishes; lower panels, representative microscopic fields. **(B)** The mRNA levels of three adipocyte marker genes, *Pparg2, Fabp4* and *Cebpa*, were examined through RT-qPCR in both preadipocytes and mature adipocytes and then normalized to *36B4.* These results are the averages of three independent RT-qPCR assays, and the error bars indicate standard deviations.

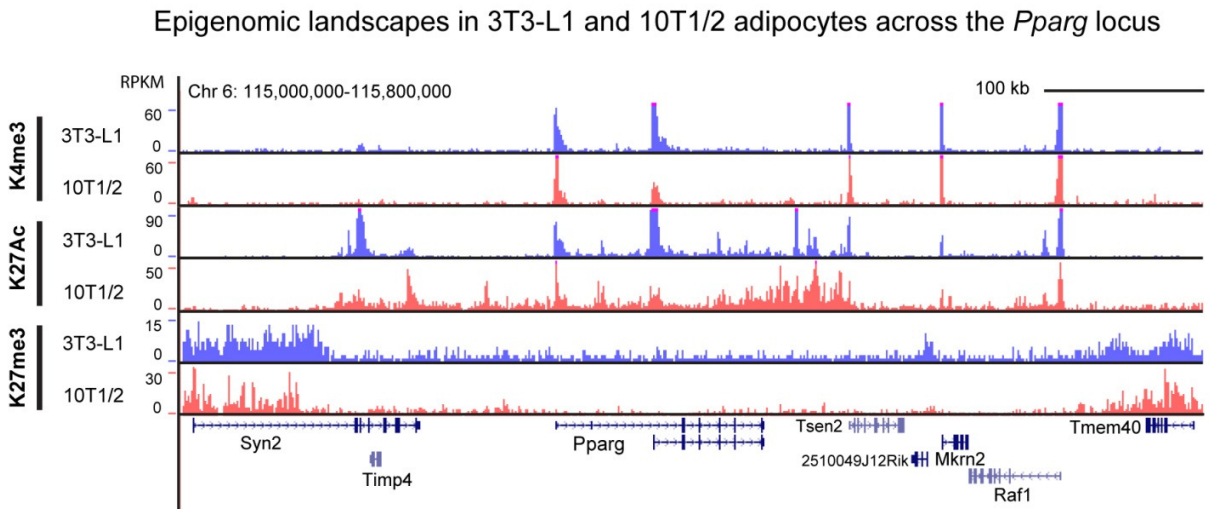

Figure S3. Epigenomic landscapes in mature adipocytes derived from 10T1/2 cells and 3T3-L1 cells.

Chromatin states of H3K4me3, H3K27ac and H3K27me3 in mature adipocytes derived from 10T1/2 cells and 3T3-L1 cells (7) across the *Pparg* locus. Epigenomic landscapes in 10T1/2 and 3T3-L1 cells were generated through the TELP and the standard Illumina protocol, respectively.

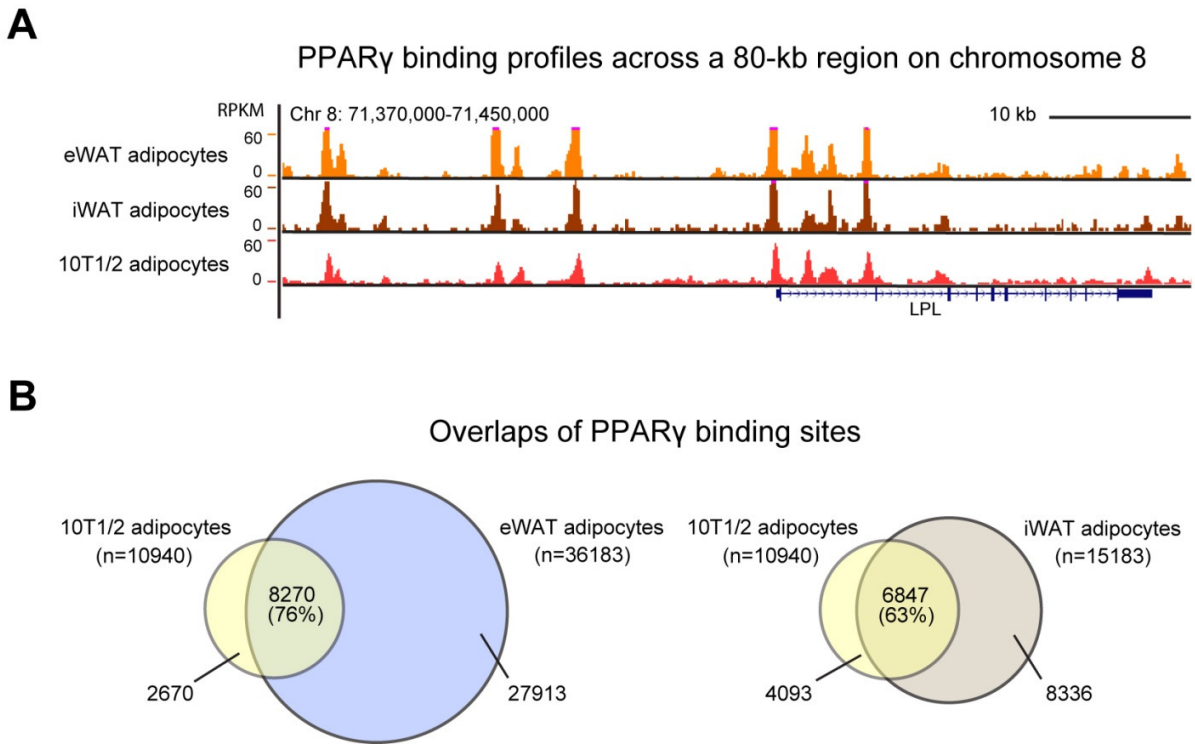

Figure S4. PPARγ binding map generated by TELP in mature adipocytes.
(A) A comparison of PPARγ binding profiles near the *LPL* gene in mature adipocytes derived from 10T1/2 cells or from progenitor cells isolated from eWAT and iWAT (12). **(B)** Venn diagrams showing overlaps between PPARγ binding peaks in 10T1/2 adipocytes and eWAT or iWAT adipocytes.

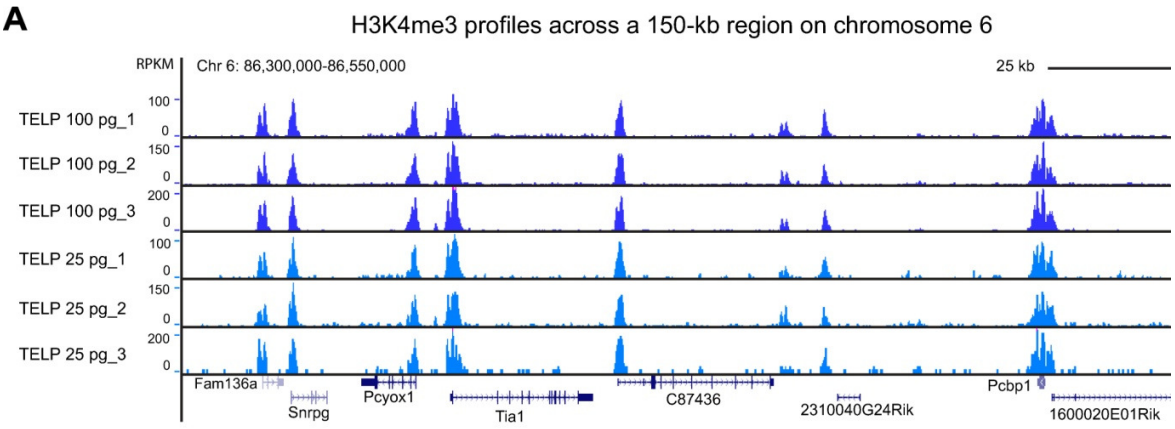
A
H3K4me3 profiles across a 150-kb region on chromosome 6
RPKM
Chr 6: 86,300,000-86,550,000
25 kb
TELP 100 pg_1
TELP 100 pg_2
TELP 100 pg_3
TELP 25 pg_1
TELP 25 pg_2
TELP 25 pg_3
Fam136a
Snrpg
Pcyox1
Tia1
C87436
2310040G24Rik
Pcbp1
1600020E01Rik

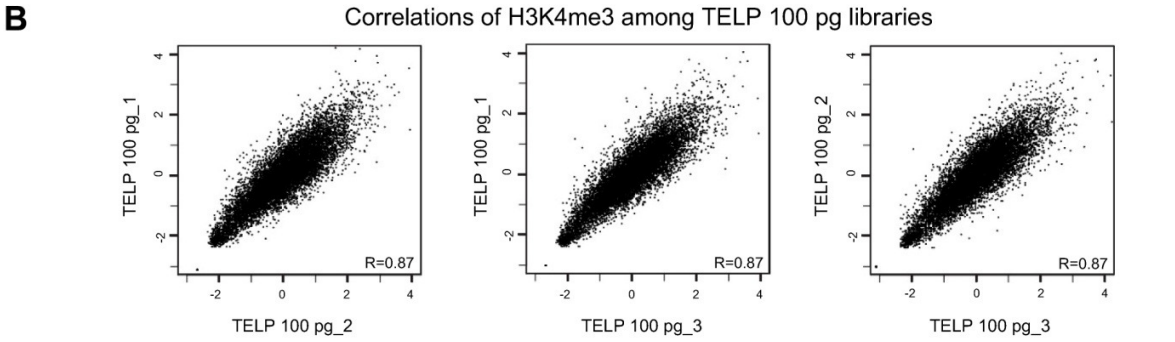
B
Correlations of H3K4me3 among TELP 100 pg libraries
TELP 100 pg_1
TELP 100 pg_2
TELP 100 pg_3
R=0.87
R=0.87
R=0.87

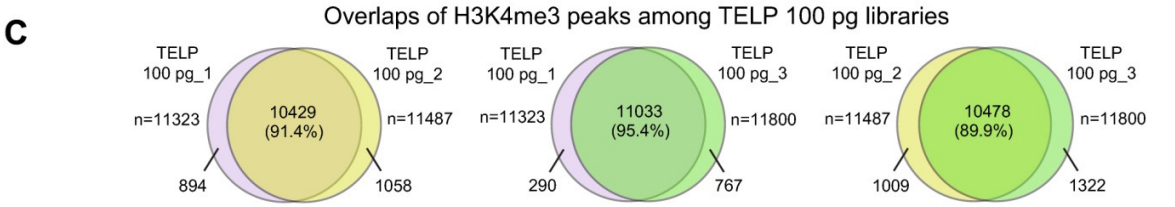
C
Overlaps of H3K4me3 peaks among TELP 100 pg libraries
TELP 100 pg_1
TELP 100 pg_2
n=11323
10429 (91.4%)
n=11487
894
1058
TELP 100 pg_1
TELP 100 pg_3
n=11323
11033 (95.4%)
n=11800
290
767
TELP 100 pg_2
TELP 100 pg_3
n=11487
10478 (89.9%)
n=11800
1009
1322

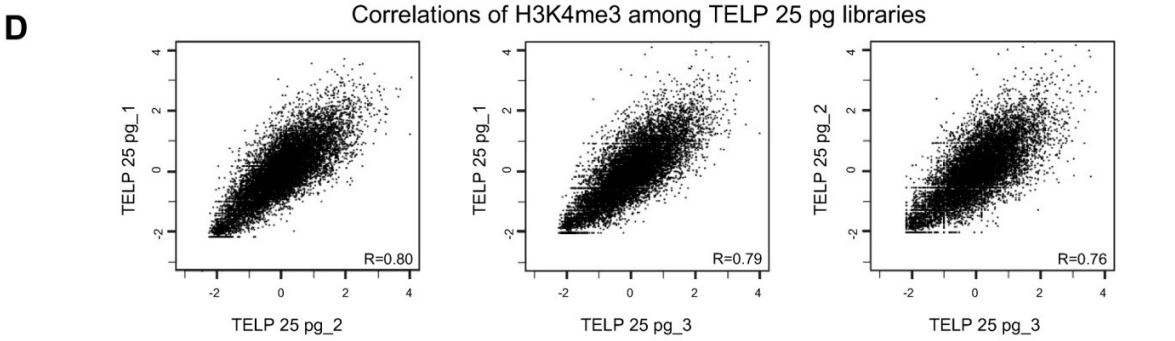
D
Correlations of H3K4me3 among TELP 25 pg libraries
TELP 25 pg_1
TELP 25 pg_2
TELP 25 pg_3
R=0.80
R=0.79
R=0.76

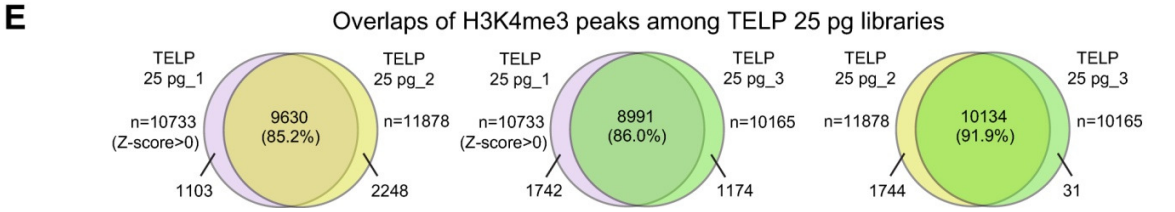
E
Overlaps of H3K4me3 peaks among TELP 25 pg libraries
TELP 25 pg_1
TELP 25 pg_2
n=10733 (Z-score>0)
9630 (85.2%)
n=11878
1103
2248
TELP 25 pg_1
TELP 25 pg_3
n=10733 (Z-score>0)
8991 (86.0%)
n=10165
1742
1174
TELP 25 pg_2
TELP 25 pg_3
n=11878
10134 (91.9%)
n=10165
1744
31

Figure S5. Reproducibility of the TELP library construction method.
(A) A comparison of the H3K4me3 TELP ChIP-seq analyses from 100 pg and 25 pg ChIP DNA (triplicates at each input level). **(B)** Scatter plots showing the pair-wise comparison of the H3K4me3 levels among the three TELP ChIP-seq analyses using 100 pg ChIP DNA. Pearson correlation coefficients, R, are indicated. **(C)** Venn diagrams showing overlaps of H3K4me3 peaks identified in the three TELP ChIP-seq analyses using 100 pg ChIP DNA. **(D)** Scatter plots showing the pair-wise comparison of the H3K4me3 levels among the three TELP ChIP-seq analyses using 25 pg ChIP DNA. Pearson correlation coefficients, R, are indicated. **(E)** Venn diagrams showing overlaps of H3K4me3 peaks identified in the three TELP ChIP-seq analyses using 25 pg ChIP DNA.

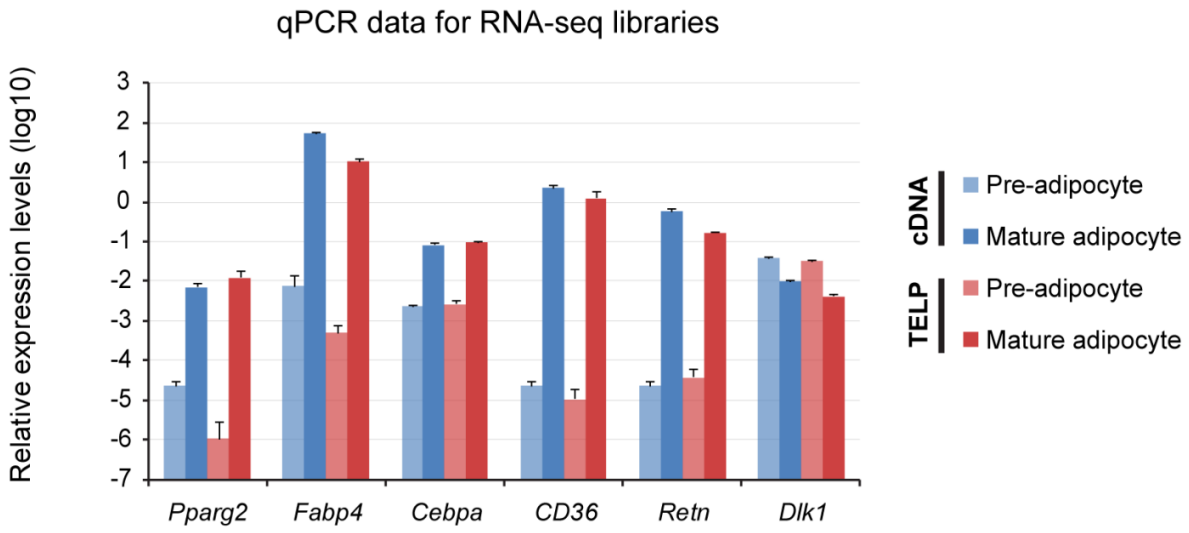

Figure S6. Validation of the TELP RNA-seq libraries by qPCR.
The expression levels of six regulatory genes of adipogenesis were determined by qPCR for original cDNAs and RNA-seq libraries prepared by TELP in preadipocytes and mature adipocytes. The data were normalized to *36B4*. These results are the averages of three independent qPCR assays, and the error bars indicate standard deviations.

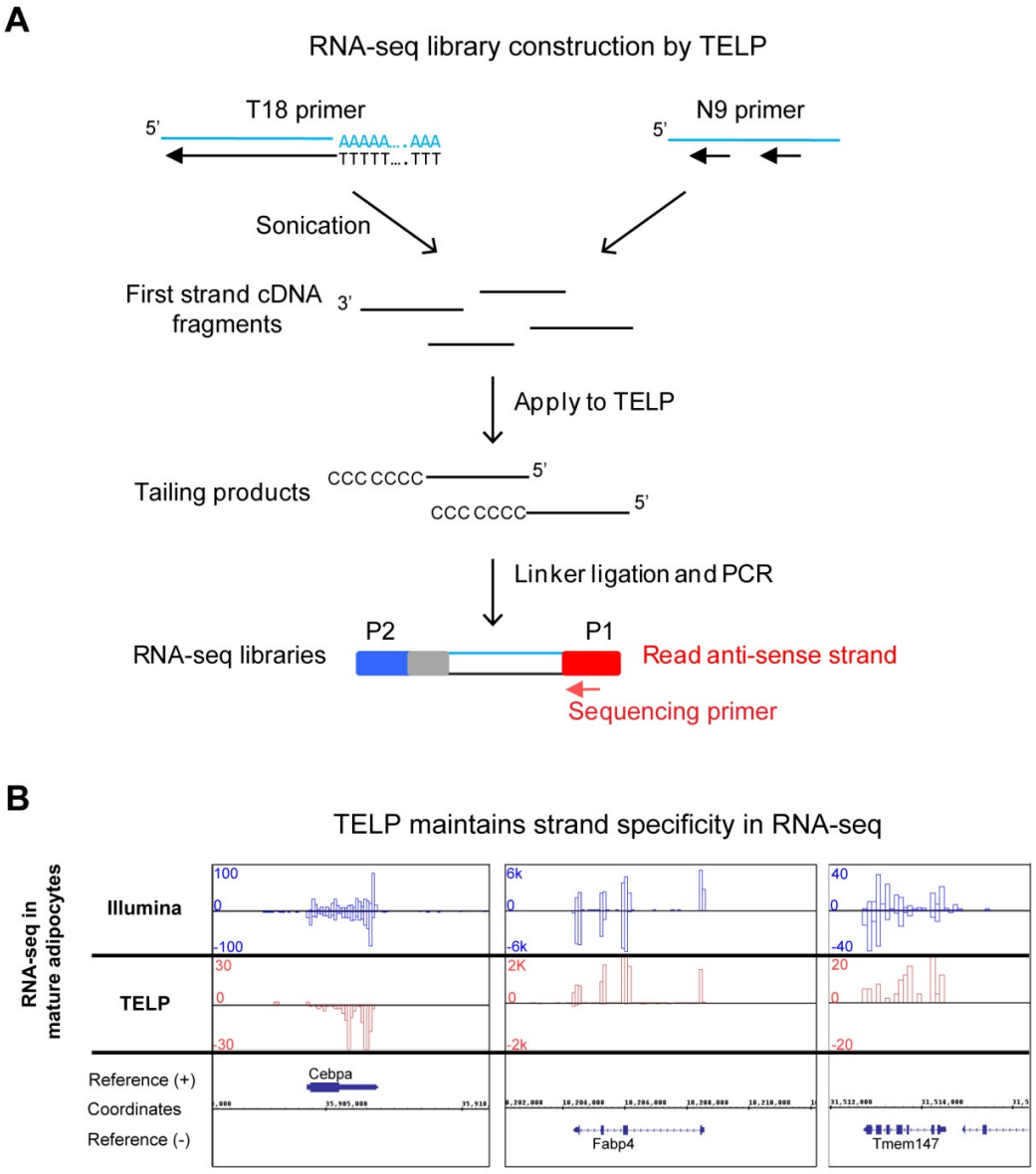

Figure S7. Strand-specific RNA-seq library preparation by TELP.
(A) A schematic of the strand-specific RNA-seq library preparation method. Poly-A RNA was reverse transcribed using a poly-T primer (T18) to generate the first-strand cDNA. Then, the single-stranded cDNA was sonicated to obtain fragments of the proper size. Alternatively, the first-strand cDNA was generated using a random N9 primer. These cDNA fragments were subsequently used as starting material for a TELP sequencing library. Finally, sequencing of the strand-specific RNA-seq library was performed on the Illumina HiSeq2000 platform in the direction indicated in the figure. **(B)** A comparison of strand-specific and non-specific RNA sequencing using the TELP and Illumina standard protocols, respectively.